Cardiff Model Utilization for Predicting the Response of Multiple-Input Power Amplifiers

Ehsan M. Azad, Roberto Quaglia, Kauser Chadhary, James J. Bell, and Paul J. Tasker
Cardiff University, Cardiff, UK (mailto: azadem@cardiff.ac.uk)

***Abstract*—This paper explores the use of the Cardiff nonlinear behavioral model to characterize the response of multiple-input power amplifiers. In particular, a case study is presented on a 300 W load modulated balanced amplifier operating at 2.1 GHz. The model mathematical formulation is presented, and the comparison between original data and model shows an error below 3%. More importantly, it is shown that the model can accurately interpolate between characterization points allowing a reduction of up to 96% of the points needed to accurately predict the model behavior. This significantly reduces the simulation and measurement time for multiple-input PA's whilst attempting to determine the optimal driving conditions.**

***Index Terms*—Power amplifier, behavioral modeling, nonlinear modeling, adaptive phase alignment.**

I. Introduction

MODERN communication signals have a very large peak to average power ratio to increase their spectral efficiency. This requires the use of advanced power amplifier (PA) architectures to provide amplification with good energy efficiency. Most of these architectures make use of multiple transistors interacting non-linearly. The most popular of these solutions is the Doherty PA [1], which is almost a standard choice in narrowband base-station transmitters. The more recently introduced load modulated balanced amplifier (LMBA) [2], [3] and some of its variants, like the inverted-LMBA, have demonstrated a better ability to operate on wider frequency bands.

Independently from the architecture of perspective, there are important advantages from a performance point of view if the multiple transistors can be driven by independent RF inputs, rather than derived from a single input by means of passive signal splitters. In fact, the so-called Multiple-Input, Single Output (MISO) PAs allow a "digital" signal splitting at baseband level, with the possibility of imposing non-linear relations between the several inputs which can help to optimize the RF performance [4], [5].

Increasing the number of inputs means increasing the degrees of freedom in using the PA, so the search for an optimum configuration of the input signals becomes an interesting engineering problem.

For MISO PAs, the search for the optimum input configuration, either directly in measurement or with a circuit level simulation, can be very time consuming. Therefore, a behavioral model extracted on a few characterization points that can still provide reasonable results on a denser exploration of the results is of great interest. For instance, work in [6] proposes a behavioral model based on expansion of multiple-input, multiple-output Voltera theory [7] for system level simulation of a PA with two input signal.

For this paper, we propose using the Cardiff behavioral model to represent the response of a dual-input inverted LMBA. After presenting the mathematical formulation used for the model, we will analyze the characterization data with different density of points, to understand what is the minimum set needed to accurately model the PA.

II. Cardiff Model

The Cardiff model is a polynomial mathematics formulation in the A-B wave domain, formed around a large signal operating point (LSOP). It describes the device outgoing phasor $B_{P,h}$ in terms of phase and magnitude of incoming phasor $A_{P,h}$ (where 'p' is the port index and 'h' is the harmonic index, referenced to the fundamental frequency f_0). The model mathematical development is based on the general mixing theory to account for the fact that when multiple CW harmonically related stimuli are injected into a multi-port nonlinear system they interact ("mix") [8].

A classic application of the Cardiff model is to extract a nonlinear model from the nonlinear measurement (usually load pull) data [9], [10]. The model coefficients are then imported within a nonlinear computer-aided design CAD simulator to be used for the design of a PA. In addition, the model is also used in algorithms of active load-pull measurement system for the development of high-speed load-pull measurement systems [11].

Due to the generality and flexibility of the Cardiff model's mathematical formulation, it can be adopted for other unconventional applications, such as predicting the response of a MISO PA. In fact, its general formulation can be used to predict the response of any multi-port nonlinear system where at least two stimulus signal, with varying phase and magnitude, are interacting.

For the case of the MISO PAs, where the goal is to model the device's single output response ($B_{3,1}$ and $B_{3,0}$) to the varying two input stimulus signals ($A_{1,1}$ and $A_{2,1}$), the Cardiff model mathematical formulation in (1) can be used [9].

$$B_{p,h} = (\angle A_{1,1})^h \cdot \sum_x \sum_m \sum_n \ldots, K_{p,h,m,n,x} \cdot |A_{1,1}|^x \cdot |A_{2,1}|^m \cdot (\angle \frac{A_{2,1}}{A_{1,1}})^n \quad (1)$$

Where the phase exponent parameter, 'n', can range from $-\infty$ to $+\infty$ and the corresponding magnitude exponents,'m' and 'x', can range from 0 to $+\infty$. Note, in this instance, as the output of the PA is matched to 50 Ω, the effect of the reflected signal at the output is ignored ($A_{3,1} = 0$).

As shown in (1), the model is normalized to the phase of the fundamental frequency at port 1 ($\angle A_{1,1}$). This phase normalization establishes a time shift to ensure that each harmonic aligns when the phase of the fundamental is 0 °. Therefore, the model coefficients are only dependent on $|A_{1,1}|$, and not the $\angle A_{1,1}$. This not only simplifies the model's mathematical formulation, it also enforces the time invariance of the model [12].

III. Verification

A. Data collection strategy

To verify the Cardiff model formulation in (1), the data was collected from simulations of a 300 W inverted-LMBA at 2.1 GHz. The Auxiliary PA (biased in class C) consists of two 170 W GaN HEMTs [13] in balanced configuration. For the Main PA (biased in class AB), a 40 W GaN HEMT [14] is used. Fig. 1 shows the block diagram of the inverted-LMBA.

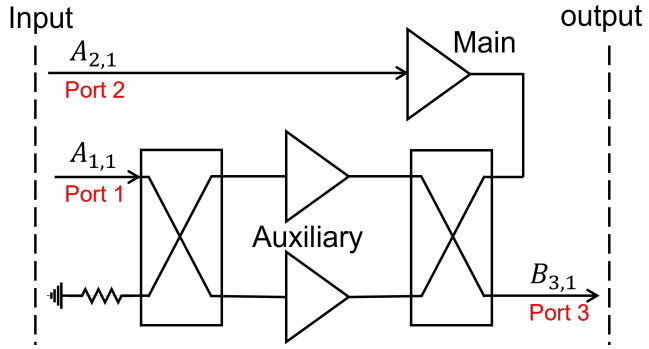

Fig. 1. Block diagram of a MISO PA with two inputs and one output. The Cardiff model formulation can be used to predict the PA's output response $B_{3,1}$ respective to the two input stimulus signals, $A_{1,1}$ and $A_{2,1}$.

As shown, separate input ports are used for the Auxiliary (port 1) and Main (port 2) PA. The input stimulus signals $A_{1,1}$ and $A_{2,1}$ are injected into the port 1 and 2, respectively. The device response at the output (port 3) is represented by $B_{3,1}$.

As only the relative phase between the two input trajectory ($\angle A_{2,1}/A_{1,1}$) is required, the "measurement" data, the $\angle A_{1,1}$ was fixed at 0 ° and only data at different $|A_{1,1}|$ was collected. With regard to the trajectory at port 2, both magnitude and phase of the $A_{2,1}$ were swept. Initially smaller data points with total of '$N_1 = 26 \times 276 = 7562$' were used (where '26' and '276' are the number of $|A_{1,1}|$ and $A_{2,1}$ sweep points, respectively) . The model's interpolation capability was tested using a larger dataset with '$N_2 = 79 \times 2412 = 190548$' points. The simulation time between the two data sets increased almost proportionally to the increase of number of points.

B. Model verification against "measurement" data

The normalized mean square error (NMSE) (2) is used to investigate the accuracy of the model and validate it across all the dataset. Fig. 2 (a) shows the calculated NMSE (dB) value for both $B_{3,1}$ and $B_{3,0}$ (for DC current (h=0) the term '$B_{3,0} \triangleq I_{3,0}$') vs. input drive level (P_{av}). Each data point on the graph represents the deviation of the model from measured dataset at specific P_{av} level. Fig. 2 (b) and (c) show a comparison between the measured and modeled $B_{3,1}$ and $B_{3,0}$, respectively, while $|A_{1,1}| = max$.

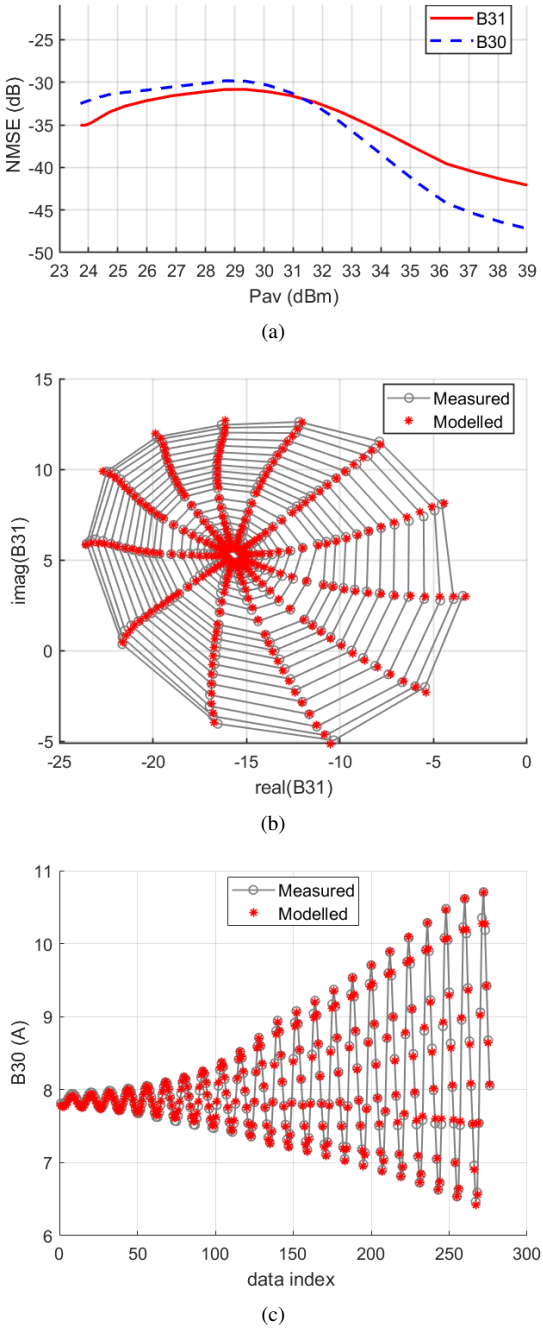

Fig. 2. Comparison of modeled and measured data. (a) NMSE (dB) vs P_{av}, and (b) measured vs. modeled $B_{3,1}$; (c) measured vs. modeled $B_{3,0}$. The model was generated from the smaller dataset '$N_1 = 7562$'.

As shown in Fig. 2 the model is capable to accurately predicting the device response with an NMSE value of less

than -30 dB, with NMSE defined as:

$$NMSE = \frac{\sum_i |B_{p,h}^{Measured} - B_{p,h}^{Modeled}|^2}{\sum_i |B_{p,h}^{Measured}|^2} \quad (2)$$

In terms of percentage, this is only a 3% deviation between the modeled and measured dataset.

C. Interpolation verification

One of the main advantage of using a behavioral model is is that there is a significant reduction in the size of the required dataset due to the interpolation between the measured points. In order to verify this capability of the model, the larger dataset with $N_2 = 190548$ points was tested using the model coefficients extracted only from $N_1 = 7562$. Fig. 3 (a) shows the NMSE (dB) value for $B_{3,1}$ and $B_{3,0}$ over the range of P_{av}; Fig. 3 (b) and (c) shows a comparison between the modeled $B_{3,1}$ and $B_{3,0}$ while $|A_{1,1}| = max$.

As shown in Fig. 3, the model is capable to accurately interpolating the measured data with NMSE value of less than -30 dB. In this example, the total number of required data points to model the device behavior was reduced from '190548' to '7562'. this is more than a 96 % reduction in the required dataset's density.

IV. Optimum Input Trajectory

The model's prediction of the device output response respective to the input stimulus signals can be used to identify the optimum input trajectory (e.g., to achieve the maximum efficiency). Fig. 4(a) shows the power added efficiency (PAE) vs. output power. The grey cloud of points shows all the possible combination of the inputs, while the solid line highlights the maximum PAE that can be achieved by properly selecting the inputs. Fig. 4(b) shows the input settings that lead to the optimum PAE, specifically the relative phase ($\angle A_{2,1}/A_{1,1}$), and the available power at the two inputs. Finally, Fig. 4 (c) the gain vs. output power with highlighted the gain resulting from selecting the input settings for optimum PAE.

As shown in Fig. 4 (a), if the 'Optimum' trajectory is selected, PAE of more than 50 % can be achieved at 10 dB output back-off (OBO), with peaks of around 67 % at both maximum power level and 7 dB OBO level. As expected, to achieve this optimal performance, a phase shift at the input is required in the OBO region (from around 60 ° to around 120 °), as shown in Fig. 4 (b). This type of power-dependent phase offset was also reported for the dual input Doherty PA in [15], where a digitally controlled adaptive phase alignment at the input is proposed. As shown in Fig. 4 (c) the optimal PAE is achieved by a compromise in the gain performance. Depending on the application and requirements a different set of combinations can be used, for example if maximum gain is required than different ($\angle A_{2,1}/\angle A_{1,1}$) can be selected.

V. Conclusion

The Cardiff behavioral model can be used to accurately predict the output response of a MISO PA to the input stimulus signals. The model coefficients can be used to interpolate between the measurement data, hence, significantly reducing the required data when trying to identify the optimal driving conditions. In this paper, the model has been verified, using the simulation data of a 300 W inverted-LMBA with NMSE value of less than -30 dB. The model shows the dataset needed to

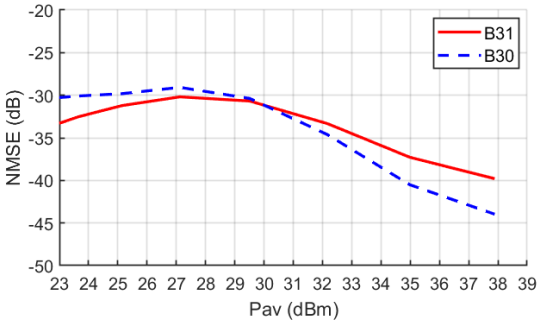

(a)

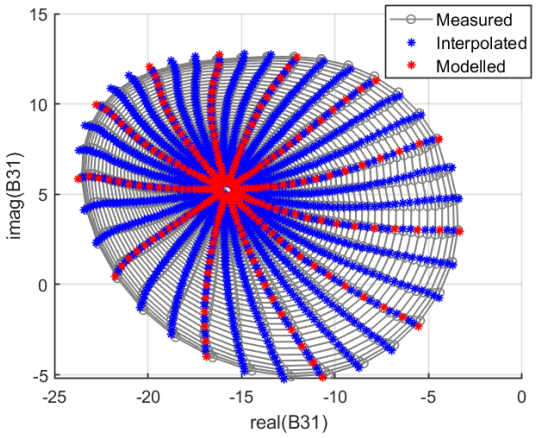

(b)

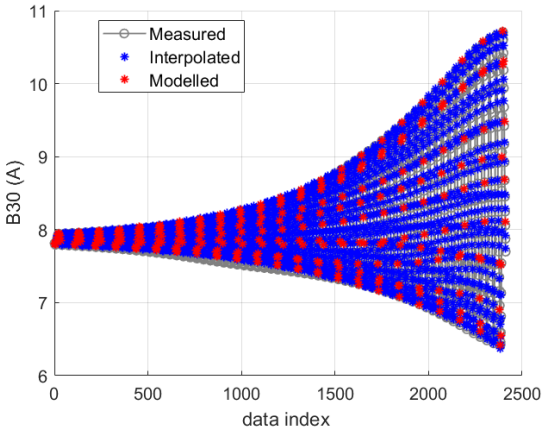

(c)

Fig. 3. Comparison of measured and interpolated dataset. (a) NMSE (dB) vs. P_{av} (dBm), (b) comparing the interpolated and modeled $B_{3,1}$ at $P_{av} = max$. The model was generated from the smaller dataset '$N_1 = 7562$' which is capable to predict a a larger dataset '$N_2 = 190548$'. This means a 96 % reeducation in the density of the required dataset via interpolation capability of the model.

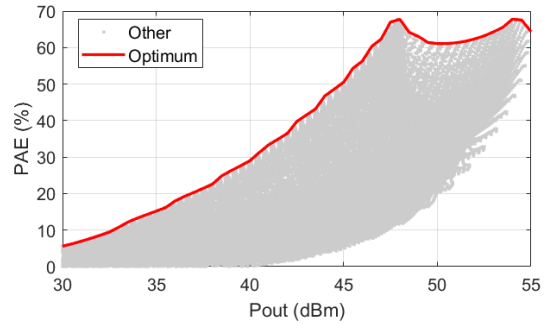

(a)

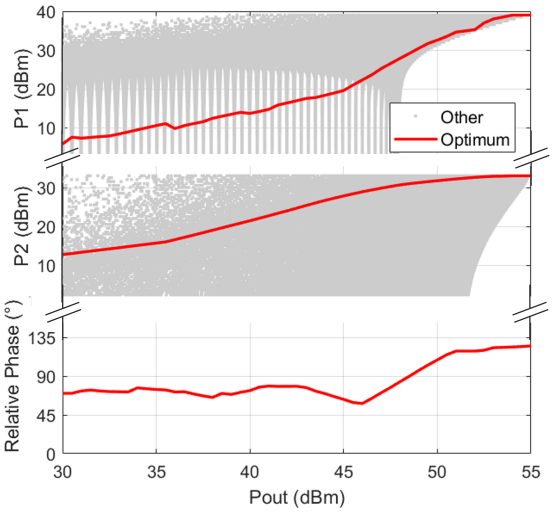

(b)

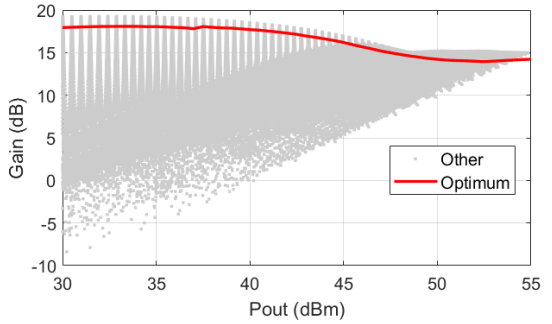

(c)

Fig. 4. (a) PAE(%) vs. output power; (b) Relative phase between the two input drives ($\angle A_{2,1}/A_{1,1}$) vs. output power (P1 (dBm) and P2 (dBm) are available powers at port 1 and 2, respectively); (c) Gain vs. output power. The 'Optimum' refers to the data points with highest PAE(%) value at each output power level, where 'Other' refers to the rest of the dataset.

accurately predict the original dataset can be reduced by 96 % while still maintaining a good accuracy.

VI. Acknowledgment

The authors would like to thank Dr Anh Nghiem and Komo Sulaksono from Ampleon Netherlands B.V. for supporting and funding this work in the context of PhD research project.

References

[1] P. Colantonio, F. Giannini, R. Giofre, and L. Piazzon, "The AB-C Doherty power amplifier. part I: Theory," *International Journal of RF and Microwave Computer-Aided Engineering*, vol. 19, pp. 293–306, 2009. doi: 10.1002/mmce.20350

[2] R. Quaglia and S. Cripps, "A load modulated balanced amplifier for telecom applications," *IEEE Transactions on Microwave Theory and Techniques*, vol. 66, no. 3, pp. 1328–1338, 2018. doi: 10.1109/TMTT.2017.2766066

[3] K. Chaudhry, R. Quaglia, and S. Cripps, "A load modulated balanced amplifier with linear gain response and wide high-efficiency output power back-off region," in *2020 International Workshop on Integrated Nonlinear Microwave and Millimetre-Wave Circuits (INMMiC)*, Conference Proceedings, pp. 1–3. doi: 10.1109/INMMiC46721.2020.9160205

[4] A. Barthwal, K. Rawat, and S. K. Koul, "Dual input digitally controlled broadband three-stage doherty power amplifier with back-off reconfigurability," *IEEE Transactions on Circuits and Systems I: Regular Papers*, vol. 68, no. 4, pp. 1421–1431, 2021. doi: 10.1109/TCSI.2021.3050543

[5] W. Shi, S. He, J. Peng, and J. Wang, "Digital dual-input doherty configuration for ultrawideband application," *IEEE Transactions on Industrial Electronics*, vol. 67, no. 9, pp. 7509–7518, 2020. doi: 10.1109/TIE.2019.2944095

[6] H. Zargar, A. Banai, and J. C. Pedro, "A new double input-double output complex envelope amplifier behavioral model taking into account source and load mismatch effects," *IEEE Transactions on Microwave Theory and Techniques*, vol. 63, no. 2, pp. 766–774, 2015. doi: 10.1109/TMTT.2014.2387842

[7] A. A. M. Saleh, "Matrix analysis of mildly nonlinear, multiple-input, multiple-output systems with memory," *The Bell System Technical Journal*, vol. 61, no. 9, pp. 2221–2243, 1982. doi: 10.1002/j.1538-7305.1982.tb03421.x

[8] P. J. Tasker, "Robust extraction of cardiff model parameters from appropriately tailored measured load-pull data," in *2020 IEEE BiCMOS and Compound Semiconductor Integrated Circuits and Technology Symposium (BCICTS)*, Conference Proceedings, pp. 1–5. doi: 10.1109/BCICTS48439.2020.9392942

[9] P. J. Tasker and J. Benedikt, "Waveform inspired models and the harmonic balance emulator," *IEEE Microwave Magazine*, vol. 12, no. 2, pp. 38–54, 2011. doi: 10.1109/MMM.2010.940101

[10] E. M. Azad, J. J. Bell, R. Quaglia, J. J. M. Rubio, and P. J. Tasker, "New formulation of cardiff behavioral model including dc bias voltage dependence," *IEEE Microwave and Wireless Components Letters*, pp. 1–4, 2022. doi: 10.1109/LMWC.2022.3140653

[11] T. Husseini, A. Al-Rawachy, J. Benedikt, J. Bel, and P. Tasker, "Automating the accurate extraction and verification of the cardiff model via the direct measurement of load-pull power contours," in *2018 IEEE/MTT-S International Microwave Symposium - IMS*, Conference Proceedings, pp. 544–547. doi: 10.1109/MWSYM.2018.8439581

[12] D. E. Root, J. Verspecht, J. Horn, and M. Marcu, *X-Parameters: Characterization, Modeling, and Design of Nonlinear RF and Microwave Components*, ser. The Cambridge RF and Microwave Engineering Series. Cambridge: Cambridge University Press, 2013.

[13] Wolfspeed, "CGHV60170D," 2020. [Online]. Available: https://assets.wolfspeed.com/uploads/2020/12/CGHV60170D.pdf

[14] ——, "CGHV60040D," 2020. [Online]. Available: https://assets.wolfspeed.com/uploads/2020/12/CGHV60040D.pdf

[15] R. Darraji, F. M. Ghannouchi, and O. Hammi, "A dual-input digitally driven doherty amplifier architecture for performance enhancement of doherty transmitters," *IEEE Transactions on Microwave Theory and Techniques*, vol. 59, no. 5, pp. 1284–1293, 2011. doi: 10.1109/TMTT.2011.2106137